

Fabrication of solid oxide fuel cell supported on specially performed ferrite-based perovskite cathode

Pawel Plonczak^{a,b}, Maria Gazda^a, Boguslaw Kusz^a, Piotr Jasinski^{b,*}

^a Faculty of Applied Physics and Mathematics, Gdansk University of Technology, ul. Narutowicza 11/12, 80-952 Gdansk, Poland

^b Faculty of Electronics, Telecommunication and Informatics, Gdansk University of Technology, ul. Narutowicza 11/12, 80-952 Gdansk, Poland

Received 3 September 2007; received in revised form 15 October 2007; accepted 6 December 2007

Available online 15 December 2007

Abstract

$\text{La}_{0.6}\text{Sr}_{0.4}\text{FeO}_3$ (LSF) is a promising material for cathode support application because its thermal expansion coefficient (TEC) is matching with typical electrolytes and it has sufficient level of ionic and electronic conductivity. In this paper, the LSF was used as a support for fabrication dense and nanocrystalline film of $(\text{Ce}_{0.8}\text{Gd}_{0.2}\text{O}_{1.95})$ CGO. The LSF support was fabricated by iso-axial pressing of powder, which was prepared using modified Pechini method. Several fabrication parameters were altered in order to obtain support with required density, conductivity and strength. This included different sintering temperatures, addition of pore former and variation of compaction pressure. The LSF powders were examined by X-ray diffractometry and did not show any other phases. The electrical conductivity and density of LSF supports were investigated in order to select optimal support for CGO film deposition. The electrical measurements indicated that porosity highly influence the electronic conductivity of LSF. A low temperature and cost-effective method, called net shape technique, was used to deposit CGO film on LSF. Impedance spectroscopy measurements (IS) of obtained structure showed that electrical conductivity of CGO film and calculated activation energy is in good agreement with literature data. SEM images indicated that the film has no cracks and is about $4\ \mu\text{m}$ thick.

© 2007 Elsevier B.V. All rights reserved.

Keywords: Cathode support; Gadolinium-doped ceria; SOFC; Perovskite; LSF

1. Introduction

Solid oxide fuel cells (SOFCs) are one of the modern, alternative energy sources that are gaining a lot of attention. Therefore several aspects of their technology are under continuous development including reduction of operating temperature, preparation of new materials with designed properties or adaptation of fabrication technology. This should lead to cost reduction of fabrication and improvement SOFC performance, which will allow wider fuel cell utilization.

Recent development of cathode materials led to replacement of conventional lanthanum strontium manganese perovskites $(\text{La,Sr})\text{MnO}_{3-\delta}$ (LSM) with perovskites, in which B site man-

ganese is exchanged to iron $(\text{La,Sr})\text{FeO}_{3-\delta}$ (LSF) or additionally substituted by cobalt $(\text{La,Sr})(\text{Fe,Co})\text{O}_{3-\delta}$ (LSCF). This is mainly due to its high catalytic activity of oxygen reduction, higher ionic and electronic conductivity [1,2]. Additionally, they have good compatibility of thermal expansion coefficient (TEC) with common electrolytes, like CGO or YSZ [3]. The chemical reactions at high temperatures between YSZ and perovskite occur for the LSCF, while for the LSF high resistance products were not detected [4,5].

In this paper the LSF was used as a support for CGO film deposition using low-temperature technique. The method is called net shape technology [6,7] and is a combination of colloidal suspension and polymer precursor [8] deposition methods. It is believed that low temperature deposition method helps avoiding formation of high resistance byproducts located between cathode and electrolyte. The main aim of this work is focused on mastering LSF support to obtain its designed properties and develop deposition methods to fabricate dense and thin film of CGO. In future this will result in fabrication cathode

* Corresponding author. Tel.: +48 58 3471323; fax: +48 58 3471757.

E-mail addresses: pawel@biomed.eti.pg.gda.pl (P. Plonczak), maria@mifgate.mif.pg.gda.pl (M. Gazda), bodzio@mif.pg.gda.pl (B. Kusz), pijas@eti.pg.gda.pl (P. Jasinski).

supported fuel cell, which may operate at lower temperatures due to thin electrolyte [9]. In this case the performance of SOFCs will strongly depend on the materials used as a cathode and an electrolyte, their processing and resulting microstructure.

2. Experimental

2.1. Cathode support preparation

Cathodes were made from $\text{La}_{0.6}\text{Sr}_{0.4}\text{FeO}_3$ (LSF) powders, which were obtained by modified Pechini method [10]. Metal nitrates (Sigma–Aldrich Co.) of $\text{La}(\text{NO}_3)_3 \cdot 6\text{H}_2\text{O}$, $\text{Sr}(\text{NO}_3)_2$ and $\text{Fe}(\text{NO}_3)_3 \cdot 8\text{H}_2\text{O}$ were dissolved in ethylene glycol and deionized water. The solution was stirred for 12 h at 75°C to evaporate water and obtain viscous liquid. Then it was pyrolyzed at 400°C on hot-plate. Obtained powders were sintered at different temperatures for 4 h and evaluated by X-ray diffraction (XRD). The powders, which were used for support fabrication, were firstly pre-sintered at 1050°C for 4 h and then iso-axially die-pressed into pellets. If not otherwise stated the pressure of 100 MPa was applied. Typically the thickness of LSF supports was below 1 mm. The density of the support was engineered by altering sintering temperature and compacting pressure. The density of cathode support was also changed by addition a pore former to LSF powder. For this purpose a synthetic graphite powder ($<20\ \mu\text{m}$) (Sigma–Aldrich Co.) was selected and mixed with LSF powder (15, 30 and 45 vol% of graphite) before forming the pellets. In this case the support was sintered at 1100°C .

2.2. Electrolyte film preparation

Film of $\text{Ce}_{0.8}\text{Gd}_{0.2}\text{O}$ (CGO) electrolyte, which was investigated in this paper, was prepared using net-shape method [6,7], which is combination of colloidal suspension and polymer precursor deposition techniques. Stoichiometric amounts of $\text{Ce}(\text{NO}_3)_3 \cdot 6\text{H}_2\text{O}$ (B&K Co.) and $\text{Gd}(\text{NO}_3)_3 \cdot 6\text{H}_2\text{O}$ (Sigma–Aldrich Co.) were dissolved in ethylene glycol and water. After stirring and heat-treatment, the solution was diluted with ethoxy ethanol and used as polymer precursor. The details related to polymer precursor preparation can be found elsewhere [8].

Colloidal suspension was prepared using CGO powder, which was prepared similarly as LSF powder. The solution of cerium and gadolinium nitrates was pyrolyzed and then fired at 600°C for 4 h. Colloidal suspension was obtained by mixing powder with ethylene glycol and water.

Electrolyte film was deposited on cathode by spin-coating technique. The CGO colloidal suspension was deposited at 6000 rpm on LSF cathode support and then slowly heated up to 360°C to obtain homogeneous powder skeleton layer. Next, powder was impregnated with polymer precursor by spin-coating at 3000 rpm. To obtain dense CGO film it was necessary to deposit polymer precursor from 50 to 100 times depending on support surface roughness.

2.3. Measurements

The X-ray diffraction (XRD) was employed to characterize crystalline phase of cathode material under different sintering conditions. Samples were scanned over the 2θ range from 20° to 90° with scan rate 0.6° per minute using Phillips X'Pert system with $\text{Cu K}\alpha$ radiation.

The densities of the samples were determined by Archimedes method assisted by vacuum saturation. The surface morphology, grain and pore sizes were investigated by scanning electron microscope (SEM) Philips XL30 ESEM.

Electrical conductivity of LSF support was measured using DC van der Pauw method. The measurements were performed in the temperature range from 400 to 800°C by Keithley 2400 SourceMeter. The electrical properties of CGO were estimated using ac impedance spectroscopy measurements (IS). The Solatron 1260 and Solatron 1287 electrochemical interface was employed for this task. Measurements were carried out in the temperature range from 400°C down to 200°C for the structure sintered at 800°C . The AC measurements were performed in the frequency range from 2 MHz to 1 Hz using excitation voltage of 15 mV. Above 400°C the resistance of the film was so low that it was not possible to measure it. The electrical contacts were prepared using gold (ESL 8080) and platinum (ESL 5442) pastes.

3. Result and discussions

3.1. Cathode support characterization

Fig. 1 displays the XRD spectra of LSF powder sintered at different temperatures. In all patterns main reflexes are indexed within the $\text{La}_{0.6}\text{Sr}_{0.4}\text{FeO}_3$ rhombohedral structure (JCPDS 82-1961). The width of the peaks corresponding to the LSF phase decreases with the increase of sintering temperature. It is related to crystalline grains growth and follows Scherrer theory. Below 1050°C additional peaks are present in the spectra. They are attributed to the SrFeLaO_4 phase. The amount of SrFeLaO_4 decreases with the sintering temperature and in the sample sintered at 1050°C it is lower than 1%. Similar results on related perovskite material were reported elsewhere as well [11,12]. Therefore 1050°C was selected as a minimum temperature for sintering of LSF powder. The fabrication procedure

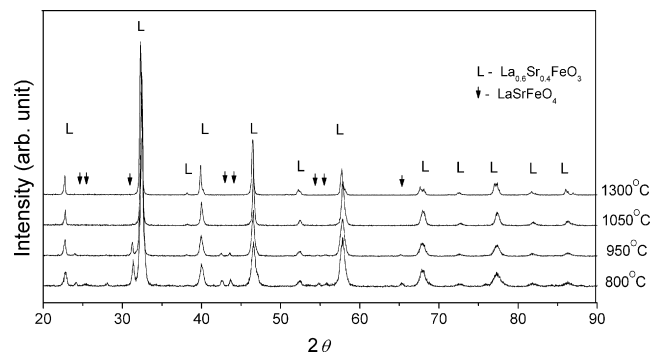


Fig. 1. XRD spectra of LSF powder sintered at different temperatures.

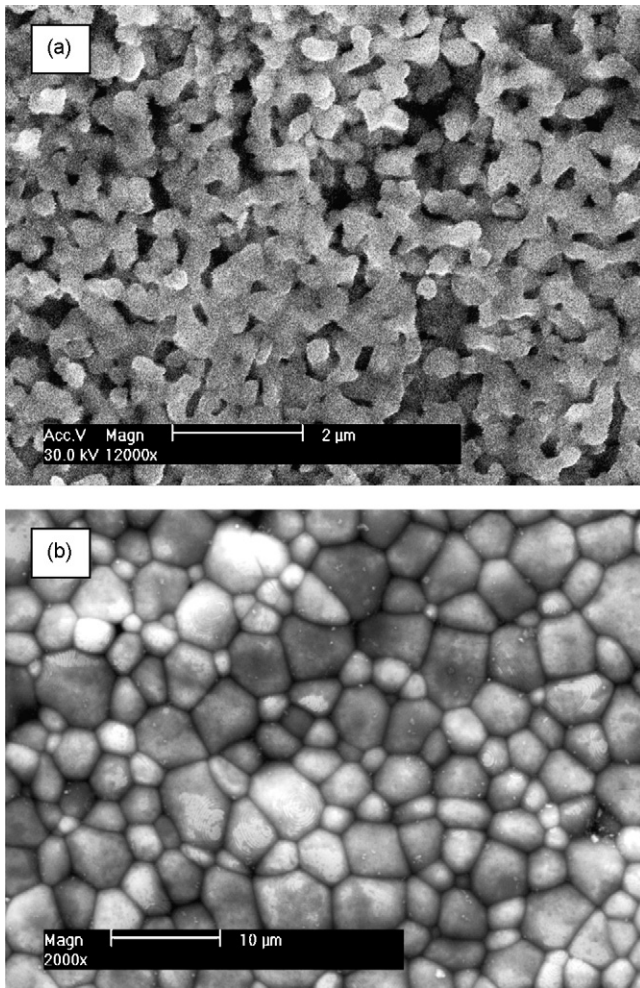


Fig. 2. SEM images of LSF supports sintered at 1100 °C (a) and 1300 °C (b).

involved pre-sintering step at 1050 °C and following iso-axial die-pressing of powders and main sintering procedure. To obtain LSF support with designed density and optimum conductivity the fabrication conditions were altered, which included different sintering temperature, pressure applied to die and pore former amount.

In Fig. 2, SEM images of LSF support sintered at 1100 and 1300 °C are presented. It can be seen that the grain size of about 0.4 and 3 μm were obtained for the samples sintered at 1100 and 1300 °C, respectively.

The electrical conductivity of LSF as a function of temperature is presented in Fig. 3a. It can be observed that maximum conductivity was obtained at about 550 °C. In case of the LSF sintered below 1200 °C the conductivity is smaller than the results taken as reference [1]. However, at the sintering temperature of 1250 °C conductivity was even slightly higher. In Fig. 3b, the electrical conductivity at 550 °C as a function of sintering temperature is presented. The lower sintering temperature the smaller conductivity was obtained. Only in case of the sintering temperature of 1300 °C a slight decrease of conductivity is observed. Up to the sintering temperature of 1250 °C the plot is linear in log-lin scale. The influence of sintering temperature on the value of conductivity most likely should be attributed to the

density of LSF, which influences the grain to grain connection. Density and grain size of LSF supports as function of sintering temperature are presented in Fig. 4. At the sintering temperature of 1050 °C the density of the LSF support of about 40% of theoretical value was obtained. While the sintering temperature was raised the density increases and more than 90% of theoretical density was obtained at 1300 °C (see Fig. 4a). The raise of sintering temperature simultaneously promotes the increase of LSF crystallites (see Fig. 4b). In case of the sintering temperature of 1050 °C the crystallites of about 100 nm were obtained. When the sintering temperature increases the crystallites grow nearly exponentially. In case of the 1300 °C the crystallites reach 3 μm.

The density of cathode supports can be also controlled by compaction pressure of LSF powder and addition of pore former to LSF powder. After several attempts the use of pore former was abandoned. This was related to the fact that the amount of

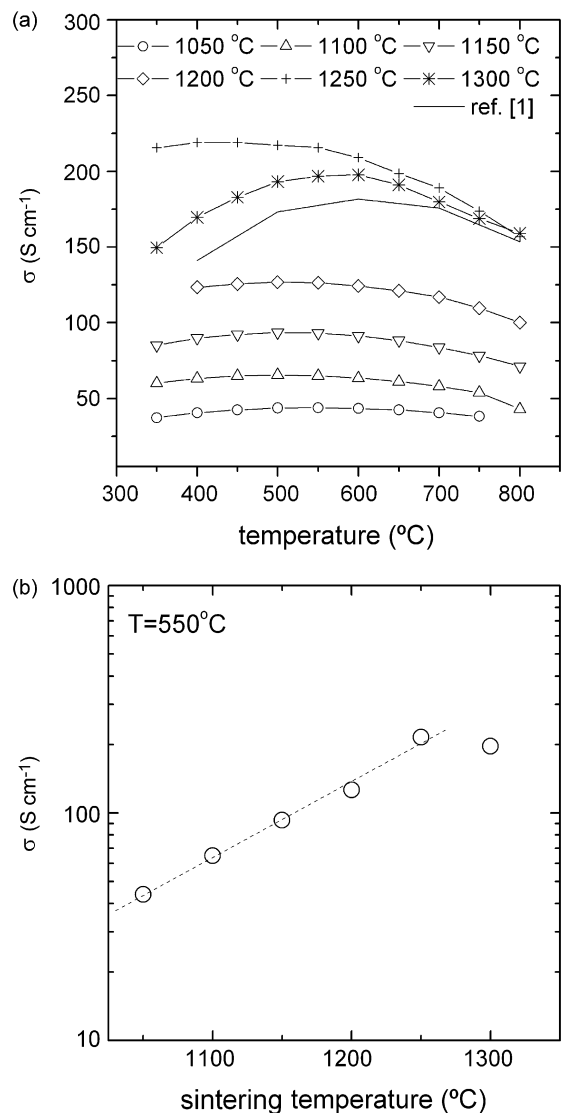


Fig. 3. Electrical conductivity of LSF as a function of operating temperature (a) and electrical conductivity of LSF at 550 °C as a function of sintering temperature (b).

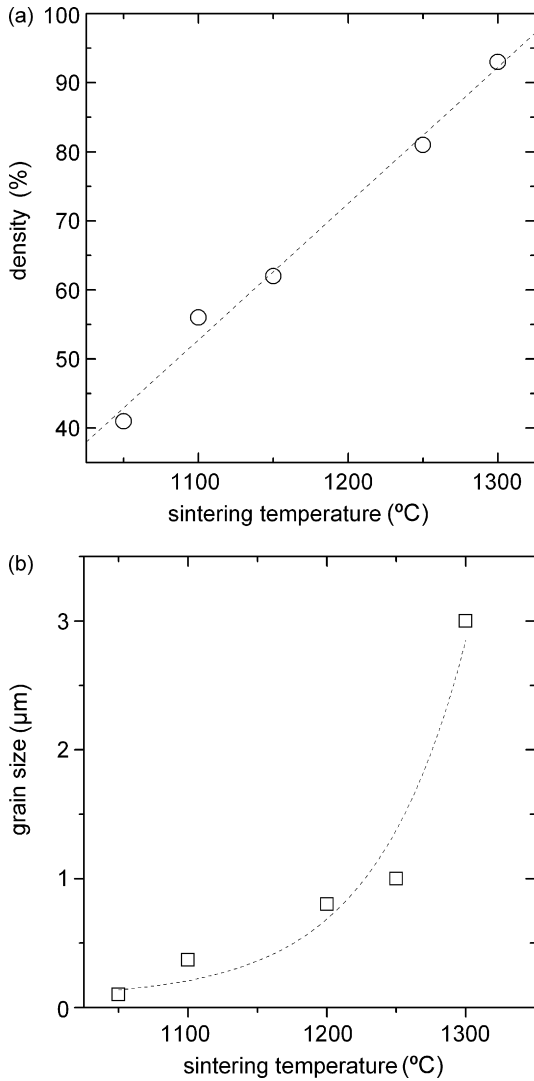


Fig. 4. Density (a) and grain size (b) of LSF supports as function of sintering temperature. The samples were obtained with 200 MPa compacting pressure.

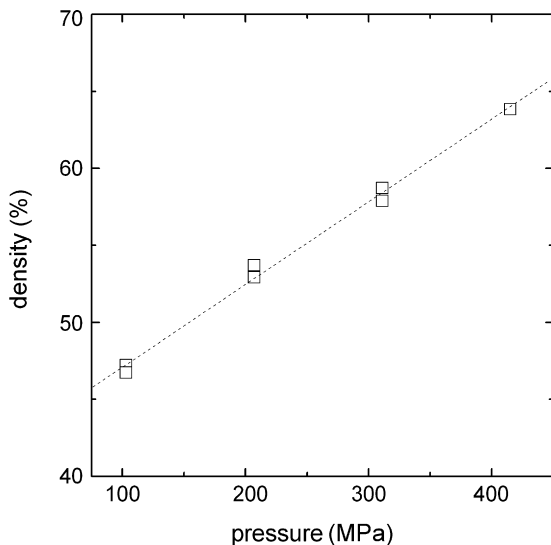


Fig. 5. Density of LSF support as a function of compacting pressure.

pore former did not significantly influence density, while the conductivity was considerably lowered. For example, in case of the 45%vol of graphite in LSF powder and use of 200 MPa compacting pressure and the sintering temperature of 1100 °C the density of 40% of theoretical was obtained, while the conductivity only of about 10 S cm⁻¹ was measured. The density can be altered as well by the variation of compacting pressure of powder. The influence of compaction pressure of LSF powder on density of LSF support sintered at 1100 °C is presented in Fig. 5. As can be predicted the density is increased when the compacting pressure is increased. In the selected range of pressures the density is changing linearly with the pressure.

Based on the results obtained from LSF support investigation it can be concluded that the density strongly influences electrical conductivity. The ideal LSF support should be porous for ease of oxygen exchange and nanocrystalline to have high catalytic activity for oxygen reduction. This can be obtained in lower sintering temperatures and lower level of compacting pressures. However, high sintering temperature is necessary to obtain high level of conductivity, which in result minimizes Ohmic resistance of cathode. Due to relatively high level of conductivity at low sintering temperatures (70 S cm⁻¹ at 1100 °C), it seems that low density (high porosity) should be a key factor for cathode support fabrication. This will avoid limited oxygen diffusion overpotential of cathode. Therefore, it was decided to use 100 MPa compacting pressure of powders and sintered temperature of 1100 and 1200 °C for cathode support preparation. Under those conditions the supports are mechanically durable, the density is lower than 60% of theoretical, while conductivity is about 70 S cm⁻¹.

The fabrication of electrolyte layers on LSF support requires deposition of water based solutions. Perovskites are known to be unstable in humid environments and therefore the resistance of LSF to decomposition in water was investigated. The LSF supports sintered at 1100 °C had been soaked in water under low vacuum conditions and then left in water at 70 °C

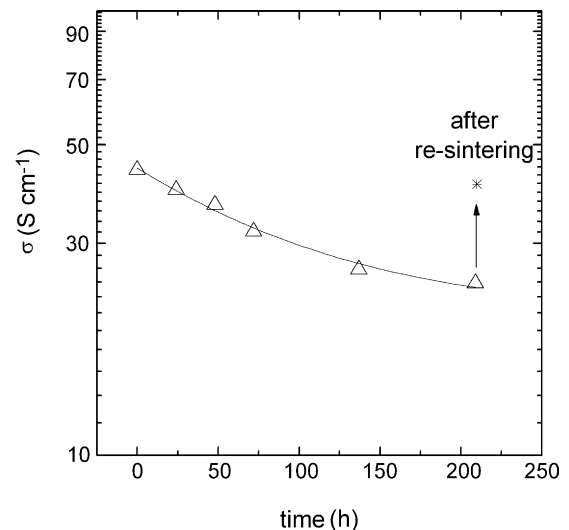


Fig. 6. Conductivity of LSF support at 550 °C as a function of soaking time in water.

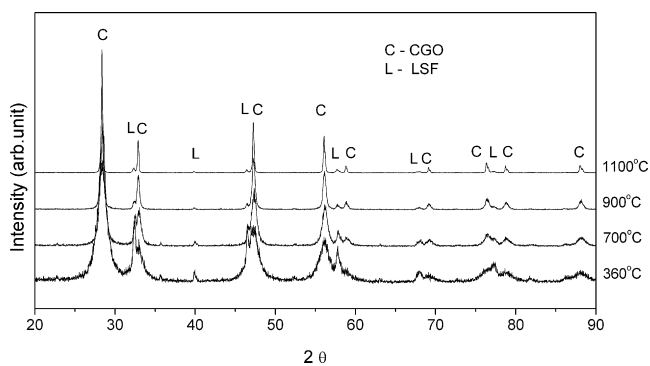


Fig. 7. XRD spectra of CGO film deposited on LSF support. The spectra of samples heat treated at higher temperatures are also shown.

for the desired time. Conductivity was measured after several hours of soaking. The results are shown in Fig. 6. The conductivity decreased by half after 200 h of soaking. However, the electrolyte deposition method does not require such long times of contact with water based precursors. Therefore only insignificant decrease of conductivity might occur. The process of perovskite decomposition is reversible. After re-sintering at 1100 °C for 4 h, the conductivity almost returned to its initial value.

3.2. Electrolyte layer characterization

The CGO film was deposited on the LSF support, which has satisfactory mechanical and electrical properties and sufficient density to act as cathode support. The properties of the CGO film on LSF were examined by SEM, XRD and impedance spectroscopy. The crystallization of CGO film was investigated by X-ray diffraction. It can be seen that XRD spectra presented in Fig. 7 contain only reflexes attributed to the cubic CGO phase and the LSF support. It means that the single phase CGO forms already at 360 °C. At higher temperatures no chemical reaction between CGO and LSF was observed. The crystallite sizes deter-

mined by Scherrer method are presented in Fig. 8. The CGO film is a composite of colloidal and polymer delivered ceria. Indeed, while analyzing XRD spectra of the CGO film it was possible to determine two kinds of the crystallite sizes. In the case of the film fired at 360 °C the crystallite sizes were estimated to be of about 7 and 30 nm. The size of ceria powder, which was used for colloidal suspension preparation, calculated from XRD spectra was of about 30 nm. Therefore it can be drawn a conclusion that the smaller crystallites are delivered from polymer precursor, while the bigger one from colloidal suspension. The colloidal suspension delivered crystallites do not increase their size up to 800 °C, while the others exponentially grow. At 900 °C the polymer precursor delivered crystallites are about 45 nm. Above 900 °C only one crystallite size can be determined from XRD spectra. The sizes of crystallites delivered from polymer precursor are in accordance with the results obtained for the ceria film prepared from polymer precursor only [13].

Fig. 9 presents SEM image of cross-section of the film—support structure. The structure was annealed at 800 °C. The CGO film is about 4 μm thick. No pinholes or cracks are observed. Even the larger pores in LSF support were covered with continuous CGO coating. The CGO layer seems to be gas-tight.

The impedance spectroscopy was employed to investigate electrical conductivity of the structure. The LSF was used as one electrode, while the second was placed on the top of CGO film. Gold and platinum electrodes were tested. The impedance spectra of the CGO film on LSF structure at 300 °C is presented in Fig. 10. Those spectra are typical for the temperature range from 400 to 200 °C. They consist of partial semicircle at high frequencies and two semicircles at middle and low frequencies. Above 400 °C the resistance related to high frequency semicircle is too low to be measured. Most likely the low frequency semicircle should be attributed to electrode overpotential and therefore is not of the interest for current study. An Arrhenius dependence of electrical conductivity, which was calculated from the high and middle frequency semicircle, is presented in Fig. 11. The high frequency semicircle is probably related to the ionic con-

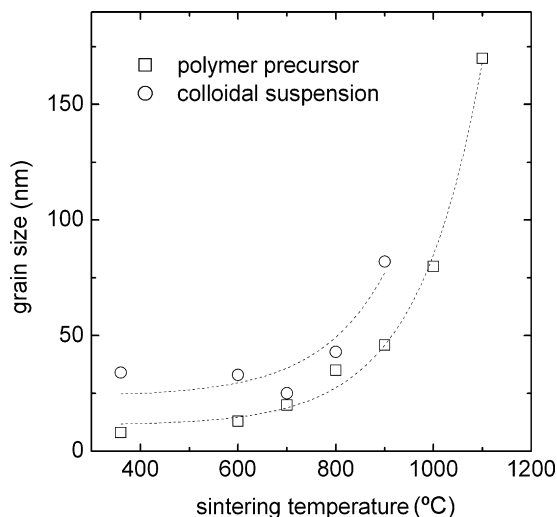


Fig. 8. The grain growth of CGO as a function of sintering temperature of CGO film on LSF. Two kinds of the crystallites were determined.

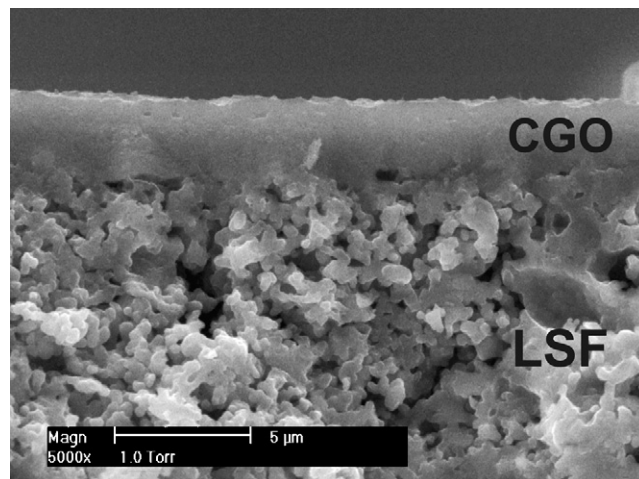


Fig. 9. SEM image of cross-section of CGO film on LSF support.

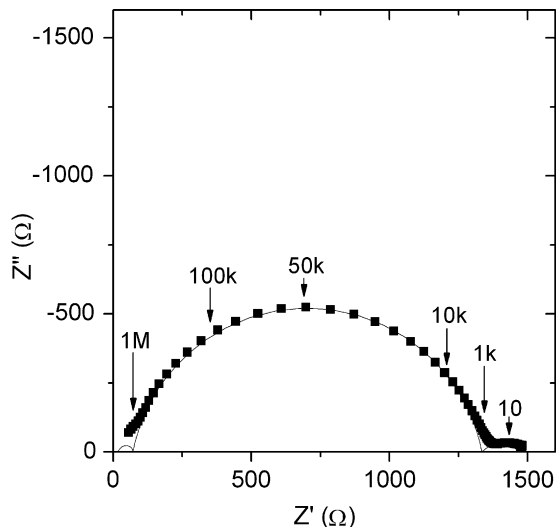


Fig. 10. Impedance spectra of CGO film on LSF at 300 °C. Numbers correspond to measurement frequency in Hz.

ductivity of ceria. The thickness of the layer calculated from the related capacitance ($C \sim 7 \text{ nF cm}^{-2}$) corresponds to the thickness of CGO film for all investigated temperatures (the dielectric constant of the layer was assumed to be 35, which corresponds to literature data of doped ceria [14]). Moreover the activation energy was estimated to be of $E_a = 0.6 \text{ eV}$ and corresponds to literature reports for the conductivity of doped ceria [15]. The level of conductivity match the data reported for ceria films deposited by colloidal suspension and polymer precursor on platinum foil [16]. However, it is a bit lower than that obtained for the films prepared by spray pyrolysis or pulse laser deposition methods [17]. The process which may be responsible for middle frequency semicircle (related capacitance $\sim 12 \text{ nF cm}^{-2}$) is most probably related to electrode overpotential. One might expect to attribute it as grain boundary conductivity. However, it is less likely because

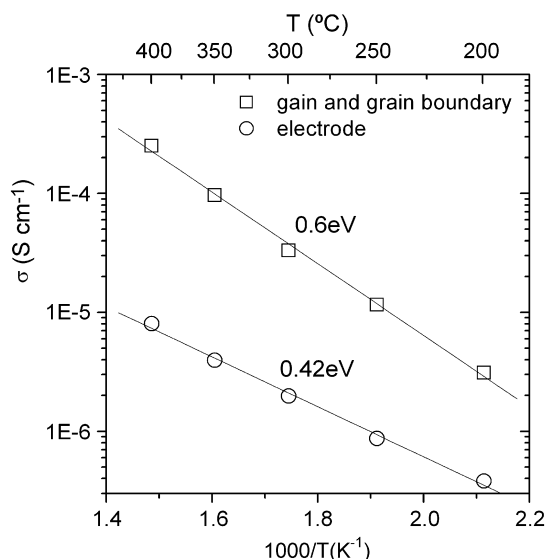


Fig. 11. Electrical conductivity of CGO film as a function of temperature.

of the value of its activation energy. The calculated activation energy of $E_a = 0.42 \text{ eV}$ is much lower than the literature data for grain boundary [15,16]. It was observed that the activation energy is of 0.77 eV for high purity microcrystalline Gd-doped ceria and from 0.8 to 1 eV for impure microcrystalline doped ceria [15]. In case of the nanocrystalline Sm-doped ceria (grain size of 40–55 nm), which was deposited by colloidal suspension and polymer precursor on platinum foil, the activation energy of 0.9 eV was obtained [16]. Therefore, it is unlikely to attribute middle frequency semicircle as the grain boundary resistance. Most likely the middle frequency arc should be attributed to electrode effect, however, currently it is not possible to explain its origin. The structure of the CGO film on LSF support is currently used for preparation fully operational SOFC, i.e. anode is being deposited on top of CGO electrolyte.

4. Conclusions

In this paper are presented results on $\text{La}_{0.6}\text{Sr}_{0.4}\text{FeO}_3$ cathode support preparation and low temperature deposition of CGO film on LSF support. The properties of the LSF support were altered by sintering temperature, powder compacting pressure and pore former. Optimal fabrication conditions (i.e. powder compacting pressure of 100 MPa and sintering temperature of 1150 °C) were used for preparation of cathode support, which was used for CGO electrolyte layer deposition. Low-temperature technique, which combines spin coating colloidal suspension and polymer precursor, allows obtaining continuous and cracked free $4 \mu\text{m}$ thick CGO layers. The electrical conductivity and activation energy of the CGO film reflects its nanocrystalline nature. It can be concluded that the investigated low temperature deposition method of electrolyte films might be useful for SOFC fabrication. The structure is currently used for preparation fully operational SOFC.

Acknowledgement

This work is supported by the project MNiSW 3 T10B 077 29.

References

- [1] H.U. Anderson, Technical Report, US Department of Energy, 2003.
- [2] H. Ullmann, N. Trofimenko, F. Tietz, D. Stöver, A. Ahmad-Khanlou, *Solid State Ionics* 138 (2000) 79–90.
- [3] V.V. Kharton, F.M.B. Marques, A. Atkinson, *Solid State Ionics* 174 (2004) 135–149.
- [4] S.P. Simner, J.P. Shelton, M.D. Anderson, J.W. Stevenson, *Solid State Ionics* 161 (2004) 135–149.
- [5] G. Stochniol, S. Broel, A. Naoumidis, H. Nickel, *Fresen. J. Anal. Chem.* 355 (1996) 697–700.
- [6] V. Petrovsky, T. Suzuki, P. Jasinski, T. Petrovsky, H.U. Anderson, *Electrochim. Solid-State Lett.* 7 (2004) A138–A139.
- [7] P. Jasinski, V. Petrovsky, T. Suzuki, T. Petrovsky, H.U. Anderson, *J. Electrochem. Soc.* 152 (2005) A454–A458.
- [8] H.U. Anderson, N.M. Nasrallah, C. Chieh-Cheng, US Patent 5,494,700, 1996.
- [9] N.Q. Minh, *Solid State Ionics* 174 (2004) 271–277.
- [10] M.P. Pechini, N. Adams, US Patent 3,330,697, 1967.
- [11] F.J. Berry, J.F. Marcob, X. Rena, *J. Solid State Chem.* 178 (2005) 961–969.

- [12] J. Liu, A.C. Co, S. Paulson, V.I. Birss, *Solid State Ionics* 177 (2006) 377–387.
- [13] I. Kosacki, T. Suzuki, V. Petrovsky, H.U. Anderson, *Solid State Ionics* 136/137 (2000) 1225–1233.
- [14] A.S. Nowick, A.V. Vaysleyb, I. Kuskovsky, *Phys. Rev. B* 58 (1998) 8398–8406.
- [15] B.C.H. Steele, *Solid State Ionics* 129 (2000) 95–110.
- [16] P. Jasinski, *Solid State Ionics* 177 (2006) 2509–2512.
- [17] J.L.M. Rupp, L.J. Gauckler, *Solid State Ionics* 177 (2006) 2513–2518.